

Thermal Characterization of High Power AlGaIn/GaN HEMTs Using Infra Red Microscopy and Thermoreflectance

Lény Baczkowski*¹, Dominique Carisetti², Jean-Claude Jacquet¹, Dustin Kendig³, Franck Vouzelaud⁴, and Christophe Gaquiere⁵

¹ III-V Lab, Route de Nozay, 91149 Marcoussis – France

² Thales Research and Technology, 1 Avenue Augustin Fresnel, 91120 Palaiseau – France

³ Microsanj, LCC, 3287 Kifer Road, 95051 Santa Clara, California – USA

⁴ Thales Systèmes Aéroportés, 2 Avenue Gay Lussac, 78990 Elancourt – France

⁵ IEMN, Avenue Paul Langevin, 59652 Villeneuve d'Ascq – France

* leny.baczkowski@3-5lab.fr

Abstract

Precise temperature knowledge is a key parameter to estimate the performances and predict the reliability of semiconductor devices. As a direct temperature measurement within a channel is most of the time not achievable, a common approach is to measure the device surface temperature and then to use simulations to estimate the channel temperature. In this paper, we propose to evaluate the interests of a new thermoreflectance thermography system, for the characterization of AlGaIn/GaN HEMTs temperature. First, this method is presented. Its advantages, such as an excellent spatial resolution associated with a short time acquisition necessary for pulsed modes, but also its limitations are then discussed. This method allows temperature measurements very close to the hot spot and then, gives a better estimation of the maximal device temperature that can be used to improve thermal simulation. We present extensive measurements performed with this method and also infra red (IR) microscopy for comparison, on multi-finger AlGaIn/GaN HEMTs, under different bias conditions. Tests and analyses have confirmed the advantages of the thermoreflectance over IR microscopy even if further analyses still have to be carried out.

1 Introduction

Over the last several years, gallium nitride (GaN) semiconductor technology has confirmed its potential to be the technology for the next generation of high frequency and high power application, thanks to its high breakdown voltage, high mobility and high current [1-3]. Furthermore, the development of high quality 4H-SiC substrates, leading to lower thermal resistance for the GaN/SiC structure, allowed to considerably increase microwave power transistors performances [4-6].

Thermal management is a key issue: with dissipated powers up to several watts per millimeters, channel temperature can rapidly exceed acceptable values. Since performances and reliability of systems depend on the devices temperature [7], an accurate estimation of this temperature is absolutely necessary: on one hand underestimated channel temperature could lead to premature failure; on the other hand, overestimated temperature could lead to unnecessary and expensive cooling systems.

As the hot spot is localized near the gate area under metallization and passivation layers, direct temperature measurement is impossible. Only simulation can provide correct temperature estimations. However, models have to be validated by measurements. A common practice is to construct a model using hypothesis, then to compare

simulation results with measurements and to refine model if necessary.

The aim of this paper is to confront a new thermoreflectance measurement system with a standard IR microscopy system [8], for the characterization of surface temperature of AlGaIn/GaN HEMTs. Extensive measurements performed with this method and also IR microscopy, on multi-finger AlGaIn/GaN HEMTs, under different bias conditions are presented. Results obtained allow validating this new characterization method.

1.1 Device and test fixture

Thermal characterization and mapping were made on an AlGaIn/GaN HEMTs grown on a SiC substrate. 8x125µm transistors in 0.25µm gate length technology have been selected for these measurements.

SiC substrates were thinned to 100µm and the chips have been soldered on 1.5 mm thick copper-molybdenum-copper carriers. Device under test (DUT) were placed onto a 15 mm thick copper test fixture. Figure 1 schematizes the different layers of the test assembly. Thermal grease was applied at the bottom of the package and at the interface between fixture and heat sink to ensure good thermal contacts.

Temperature at the bottom of the carrier is regulated with a thermal chuck and controlled with a thermocouple at +/- 0.1°C. A DC power supply and a commercial gate pulse

generator are used for both DC bias measurement and pulsed bias measurement.

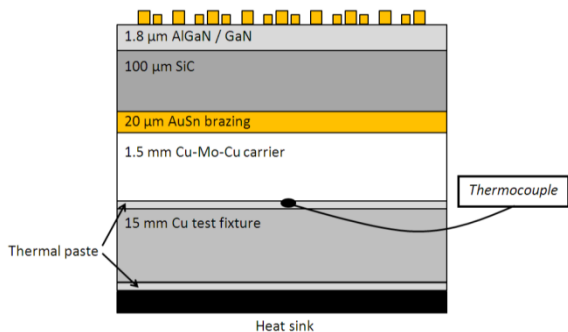


Figure 1: Schema of the test assembly

2 Thermal characterization techniques

2.1 Infrared thermography

The IR thermography measurement is obtained using a QFI brand microscope system. The samples were placed onto a 4 inch copper plate, vacuum-maintained onto a temperature controlled chuck. In DC bias measurement, an InSb 512x512 pixels camera is used to record the spectral distribution of radiations at the surface of samples and then to realize the device thermal mapping. In transient measurement, a lock-in mono pixel detector acquires dynamic evolution of the mean spectral distribution, from a small localized area. Spatial resolution of steady-state measurement is close to 2 μm at 20X magnification. In transient measurement, spatial resolution is around 20 μm , at 20X magnification.

Variations of emissivity due to material differences have to be compensated for a correct temperature measurement. Emissivity depends on material type, temperature, surface roughness and wavelength. To consider this dependence, a calibration curve of the sample is first performed and then the temperature can be extracted.

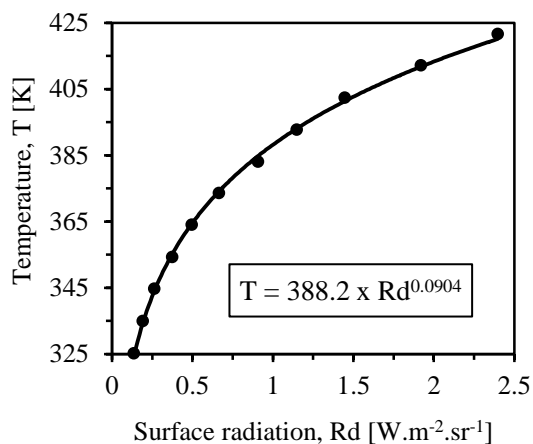


Figure 2: Results of calibration curve for InSb camera

Calibration consists in increasing temperature of non-biased sample from 50°C to 200°C with a step of 15°C and then records the surface radiation. A thermocouple placed at the bottom of the package provides the reference temperature. After calibration, thermal scans of the biased AlGaIn/GaN HEMT are performed. In order to reduce the background measurement noise, the signal is averaged over 100 to 150 scans each time.

2.2 Thermoreflectance thermography

The thermoreflectance thermography measurement is obtained using a Microsanj brand system [9], mounted on an optical table to isolate measurements from building vibrations. 1626x1236 pixels high speed camera is used to record the light reflected by the sample surface (initially emitted by a LED). Major benefit of such technique is its ability to work under visible light, allowing to achieve a spatial resolution lower than 1 μm at 50X magnification.

As reflectivity of material depends on wavelength [10-11], 3 different LEDs colours can be used: green (530nm), blue (470nm) or white. In this case, the green colour was chosen, since it was providing the best contrasted image in the observed region (drain-gate space), as shown in figures 3, 4 and 5.

As for IR microscopy, a calibration is needed in order to calculate a thermal coefficient C_{th} for a given sample surface. The thermal coefficient depends on material type, wavelength of the excitation source (LED), temperature, roughness, waviness and planarity of the sample. This coefficient is part of the relation between changes of reflectivity ΔR and temperature variation ΔT , as shown in equation 1, where R_0 is reflectivity for temperature T_0 .

$$\Delta T = \Delta R / (R_0 \cdot C_{th}) \quad (1)$$

To define the coefficient C_{th} , a Peltier cell is placed under the unsoldered die and used to progressively increase the temperature of a non-biased sample from 25°C to 65 °C, while the camera records surface reflectivity variation. The calibration had to be performed at a 5X magnification to reduce the impact of the thermal expansion on the focalization.

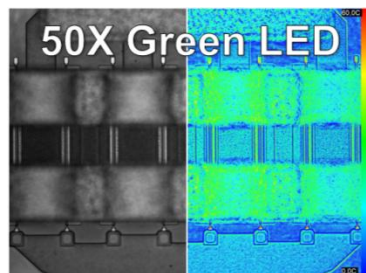


Figure 3: Thermoreflectance measurement using green LED

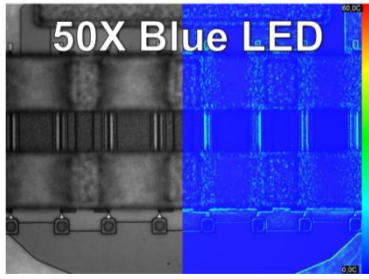


Figure 4: Thermoreflectance measurement using blue LED

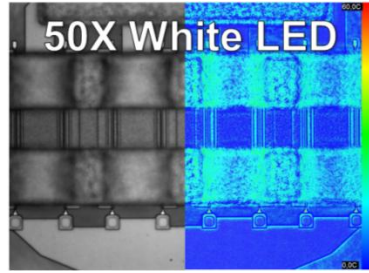


Figure 5: Thermoreflectance measurement using white LED

In order to have all gates in the same picture frame, thermoreflectance scans of the AlGaIn/GaN HEMT were performed at a 50X magnification. As the magnification used in measurement phase is different from the one used for calibration phase, temperature measurement can be misleading due to dependence between the numerical aperture and the thermal coefficient. To evaluate this effect, measurements using different magnifications have been performed on the same large gold area (typically the drain) with the same temperature. They have led to a thermal coefficient correction of -17%.

The corrected thermal coefficient value for the green LED at 50X magnification is $-2.13 \times 10^{-4} \text{ } ^\circ\text{C}^{-1}$ for passivated AlGaIn surface.

3 Temperature measurement

3.1 Steady-state (DC bias) measurement

DC bias measurements were first performed to validate both thermoreflectance system and thermal coefficient value previously determined. Temperature measurements were carried out between the gate and the drain, at the surface of the device. Temperatures were calculated, by averaging the temperatures in the gate-drain area of the two central gates. Measurements were performed on 3 samples for statistics.

The first series of DC biased measurements are gathered in tables 1 and 2. For each sample, the gate-source voltage V_{GS} has been chosen to obtain drain-source current $I_{DS}=120, 200$ and 320 mA at a drain-source voltage $V_{DS}=25\text{V}$, providing DC power densities of 3, 5 and $8\text{W}\cdot\text{mm}^{-1}$ respectively. The temperature increase $\Delta T = T_{max} - T_{baseplate}$ were extracted for both techniques and the same value of ΔT has been obtained that validate the methodology.

ΔT [$^\circ\text{C}$]	IR microscopy		
DC power	Sample 1	Sample 2	Sample 3
3W/mm	38.9	35.9	40.4
5W/mm	61.2	59.1	57.5
8W/mm	97.8	92.9	94.4

Table 1: DC power influence on thermal resistance, using IR microscopy

ΔT [$^\circ\text{C}$]	Thermoreflectance		
DC power	Sample 1	Sample 2	Sample 3
3W/mm	31.1	33.1	30.9
5W/mm	51.7	54.0	55.3
8W/mm	N.A.	97.7	101.4

Table 2: DC power influence on thermal resistance, using thermoreflectance

Second series of DC bias measurements show the values of thermal resistance $R_{th} (= \Delta T/P)$, for different baseplate temperatures $T_{baseplate}$. By increasing $T_{baseplate}$, R_{th} rises, as can be seen in tables 3 and 4. This is due to the thermal non-linearity of the semi-conductor thermal conductivity.

R_{th} [$^\circ\text{C}\cdot\text{mm}\cdot\text{W}^{-1}$]	IR microscopy		
$T_{baseplate}$	Sample 1	Sample 2	Sample 3
50 $^\circ\text{C}$	12.2	11.8	11.5
100 $^\circ\text{C}$	12.5	11.9	12.2
175 $^\circ\text{C}$	17.3	14.8	15.4

Table 3: Baseplate temperature influence on thermal resistance, measured by IR microscopy

R_{th} [$^\circ\text{C}\cdot\text{mm}\cdot\text{W}^{-1}$]	Thermoreflectance		
$T_{baseplate}$	Sample 1	Sample 2	Sample 3
50 $^\circ\text{C}$	10.3	10.8	11.1
100 $^\circ\text{C}$	15.4	14.3	13.3
175 $^\circ\text{C}$	18.9	16.9	19.1

Table 4: Baseplate temperature influence on thermal resistance, measured by thermoreflectance

3.2 Transient (pulsed bias) measurement

Only thermoreflectance transient measurements are discussed in the following section and that, for two reasons: 1 – Due to the low spatial resolution of IR thermography (around $20 \mu\text{m}$ in transient mode), temperature is averaged on materials with different emissivity and thermal properties. The few measurements performed in this mode provided inconsistent temperature results. 2 – In contrast to

IR thermography, thermoreflectance technique is able to provide thermal mapping with high spatial resolution in the sub micrometer range.

Transient measurements were performed in pulsed bias conditions. A scan is recorded at the end of each pulse when the surface temperature is supposed to reach its maximum temperature. The lowest duty cycle chosen for short pulse durations is 25%. Acquisition starts a few seconds after the first pulse, so that the fixture has reached an overall stable temperature.

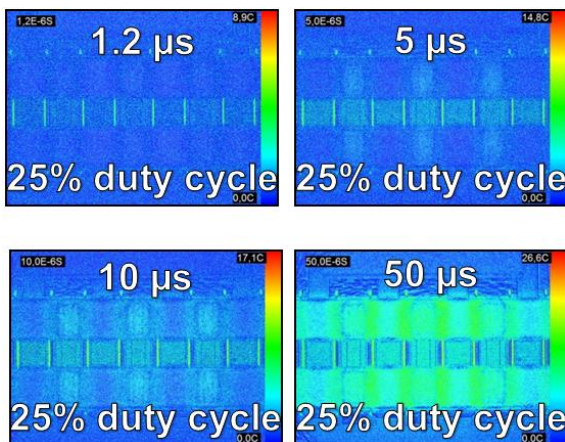


Figure 6: Transient thermoreflectance results

Figure 6, shows the device thermal mapping for different pulse lengths. The same temperature increase is measured between the different gates for a 1.2 μs pulse length. This result indicates that, at this pulse length, a uniform power is dissipated in each gate of the transistor.

4 Thermal simulation

4.1 Steady-state (DC bias) mode

3D-Simulation finite element model (FEM) was made using ANSYS commercial software. Physical simulations were firstly performed to determine the size and the location of the heat generated, as described in [12].

Thermal conductivities of materials used have been deduced from Raman measurement and the values published in [13]. Since the IR and thermoreflectance thermography techniques give the surface temperature of the DUTs, the simulated temperature was averaged at the top of the passivation layer, in order to compare values.

Figures 7 and 8 show the surface temperature mapping using IR thermography and FEM simulation respectively. A good correlation between measurement and simulation is found.

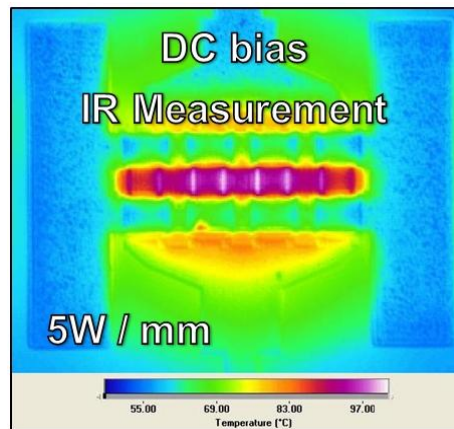


Figure 7: IR DC bias measurement results

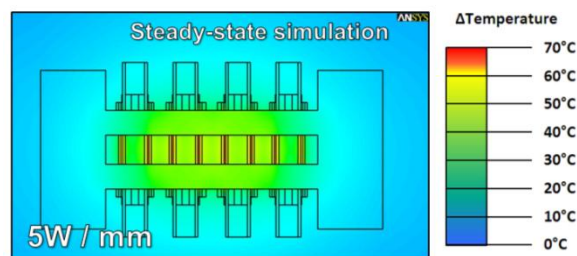


Figure 8: Steady-state simulation results

Figure 9 shows the thermal resistance of each gate of the device for the three methods. The gates temperatures have been extracted from figures 6, 7 and 8 and the associated thermal resistances R_{th} have been calculated using equation (2):

$$R_{th} = (T_{max} - T_{baseplate}) / P \quad (2)$$

where $T_{baseplate} = 50^\circ\text{C}$ and $P = 5\text{W}\cdot\text{mm}^{-1}$. T_{max} value is deduced from surface temperature value using IR thermography, thermoreflectance thermography and FEM simulation. R_{th} values determined by these three methods are in good agreement, and differ by less than 10%. Different values of thermal resistance have been found for the middle gate and the peripheral gate. This difference is due to the thermal flow pattern between the center and the external gates.

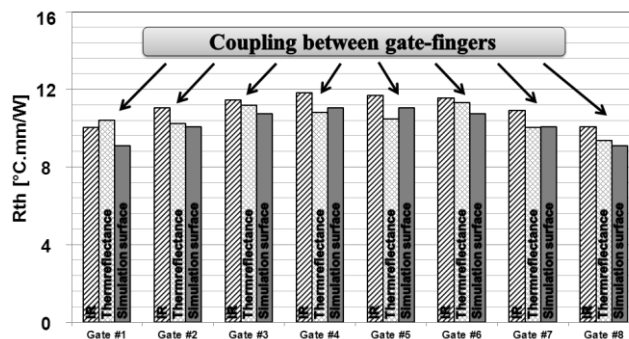


Figure 9: DC bias results comparison

Figure 10 shows a comparison of the simulated temperature in the channel (red curve) and on the device surface (green curve) for a dissipated power of $5\text{W}\cdot\text{mm}^{-1}$. A maximum temperature difference of 25°C is simulated, this corresponds to a thermal resistance which is about $5^\circ\text{C}\cdot\text{mm}\cdot\text{W}^{-1}$ higher in the channel than at the device surface. As expected, this result confirms that IR and thermoreflectance techniques cannot directly provide the maximal temperature seen by the transistor.

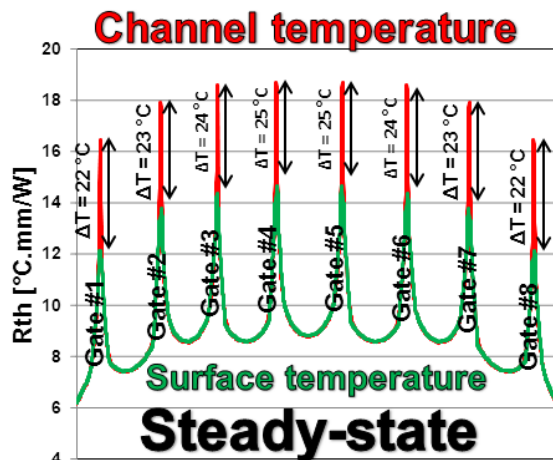


Figure 10: Temperature difference between surface and channel area

4.2 Transient (pulsed bias) mode

Figure 11 shows the temperature increases in transient mode, obtained by both simulations and measurements. A direct comparison between the 2 curves reveals a large offset obtained for short pulse lengths.

First assumption was that the transient material properties used in the simulation (density ρ and specific heat C_p), were erroneous. But the product $C_p \times \rho$ has a negligible impact on surface temperature (less than 1°C even if this product is multiplied by 1000).

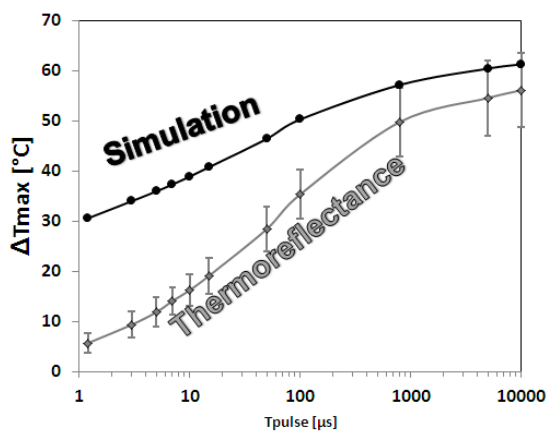


Figure 11: Transient comparison results between simulation and thermoreflectance measurements

The most probable explanation, given by Tessier et al. in [5] and [6], is that the thickness of the passivation

layer strongly impacts thermoreflectance measurement results. Because calibration was made on a larger area than the measured one (see section 2.2), the thickness of the passivation layer could be slightly different. Furthermore, other factors can modify the material reflectivity such as the surface waviness as show in figure 12, the surface roughness or a dispersion of the refractive index due to non-uniform stoichiometry of the nitride. Standard deviation calculation of temperature represented by error bars on Figure 11 has been performed, by averaging the temperature at different location in the gate-drain space area.

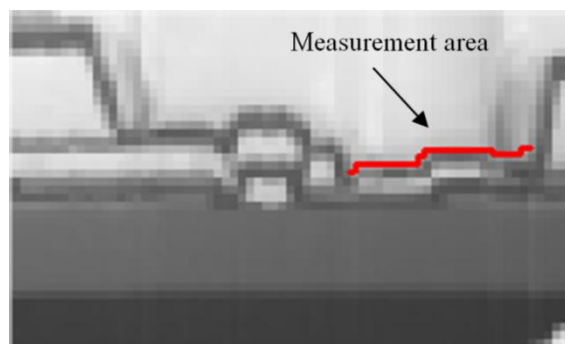


Figure 12: Slide view of the DUT

5 Discussion

Due to their high spatial resolution, IR and thermoreflectance thermography are suitable as non-invasive measurement techniques for HEMTs thermal characterization and mapping. However attention has to be paid on surface quality for both systems.

In IR thermography, emissivity difference between materials could lead to misleading temperature scattering. In thermoreflectance thermography, DUT surface planarity could modify the intensity of the reflected light and therefore affect the thermal coefficient obtained by calibration. So calibration has to be conducted with a robust protocol.

DC bias measurements show a good correlation between IR thermography, thermoreflectance thermography and FEM simulation. Similar temperatures were found by these three methods, resulting in a higher confidence in the accuracy of the in-house model.

Due to its low spatial resolution IR thermography used in transient mode is not adapted for HEMTs. On the contrary, thermoreflectance thermography has a sub micrometers spatial resolution for both DC and transient mode that allows thermal mapping of HEMT device surface with a sufficient spatial resolution.

Comparison between simulation and transient thermoreflectance highlights differences that increase with short pulse length. As explained before, planarity of sample and passivation thickness strongly impact results which could be the cause of the observed deviation. To confirm

this hypothesis and thus to reduce error, a dedicated calibration sample should be used.

6 Conclusion

In this paper, AlGaIn/GaN HEMTs thermal measurements using IR and thermoreflectance thermography technique were presented and compared to simulation using an in-house developed model.

For steady-state condition, both measurement methods and simulation provide similar results validating the thermal model in this mode. Simulation shows that IR and thermoreflectance techniques do not provide the maximum temperature seen by the transistor, and a difference of $5^{\circ}\text{C}\cdot\text{mm}\cdot\text{W}^{-1}$ between the measured surface temperature and the channel one is estimated from simulation.

For transient measurement, a temperature difference between measurement and simulation that increase with short pulse length has been observed. As the calibration is made at a magnification lower than the one used for measurements, the discrepancy could be explained by homogeneity and/or thickness differences of the passivation and may have led to error in the determination of the coefficient C_{th} . Nevertheless transient thermal mapping gives very important information about the uniformity of the power distribution between gates.

As each system has advantages and limitations depending on the bias mode chosen, thermoreflectance thermography and IR thermography must be considered as complementary methods for measurements of device surface temperatures.

Acknowledgements

The authors wish to thank UMS, for providing components and Olivier Jardel (from III-V Lab) for fruitful discussion.

Literature

[1] U.M. Mishra, L. Shen, T.E. Kazior, Y-F. Wu, "GaN-Based RG Power Devices and Amplifiers", Proceedings of the IEEE, Vol.96, no.2, February 2008.

[2] M.J. Uren, A.R. Barnes, T. Martin, R.S. Balmer, K.P. Hilton, D.G. Hayes, M. Kuball, "GaN Devices for Microwave Power Application", 10th IEEE International Symposium on Electron Devices for Microwave and Optoelectronic Applications, November 2002.

[3] R.J. Trew, L.G. Bilbro, W. Kuang, Y. Liu, H. Yin, "Microwave AlGaIn/GaN HFETs", IEEE Microwave Magazine, Vol. 6, no.1, March 2005.

[4] R.S. Pengelly, S.M. Wood, J.W. Milligan, S.T. Sheppard, W.L. Pribble, "A Review of GaN on SiC High Electron-Mobility Power Transistors and MMICs", IEEE Transactions on Electron Devices, Vol. 60, no.6, June 2012.

[5] D. Hobgood, M. Brady, W. Brixius, G. Fechko, R. Glass, D. Henshall, J. Jenny, R. Leonard, D. Malta, S. G. Muller, V. Tsvetkov, and C. Carter, "Status of large diameter SiC crystal growth for electronic and optical applications," *Silicon Carbide Rel. Mater., 1999 (Part 1) Mater. Sci. Forum*, vol. 338–342, pp. 3–8, 2000.

[6] S. T. Sheppard, W. L. Pribble, D. T. Emerson, Z. Ring, R. P. Smith, S. T. Allen, J. W. Milligan, and J. W. Palmour, "Technology development for GaN/AlGaIn HEMT hybrid and MMIC amplifiers on semi-insulating SiC substrates," in *Proc. IEEE/Cornell High Perform. Devices Conf.*, Ithaca, NY, Aug. 7–9, 2000, pp. 232–236, IEEE Cat. 00CH37122.

[7] M. Kuball, M.J. Uren, T. Martin, "Reliability optimization for wide bandgap devices: Recent developments in high-spatial resolution thermal imaging of GaN devices", 2005 International Semiconductor Device Research Symposium, December 2005.

[8] J.D. McDonald, G.C. Albright, "Microthermal imaging in the infrared", *Electron. Cooling*, vol.3, no.1, pp.26-29, January 1997.

[9] K. Yazawa, D. Kendig, D. Hernandez, K. Maze, A. Shakouri, "Challenges and opportunities for transient thermal imaging of microelectronic devices", 18th International Workshop on Thermal Investigations of ICs and Systems (THERMINIC), pp. 1-4, September 2012.

[10] G. Tessier, S. Holé, D. Fournier, "Quantitative Thermal Imaging by Synchronous Thermoreflectance with Optimized Illumination Wavelengths", *Applied Physics Letters*, Vol. 78, no.16, April 2001.

[11] G. Tessier, G.Jerosolimski, S. Holé, D. Fournier, C. Filloy, "Measuring and Predicting the Thermoreflectance Sensitivity as a Function of Wavelength on Encapsulated Materials", *Review of Scientific Instruments*, Vol.74, no.1, January 2003.

[12] R. Aubry, J.-C. Jacquet, J. Weaver, O. Durand, P. Dobson, G. Mills, M.-A. di Forte-Poisson, S. Cassette, S.-L. Delage, "SThM Temperature Mapping and Nonlinear Thermal Resistance Evolution with Bias on AlGaIn/GaN HEMT Devices", *IEEE Transactions on Electron Devices*, Vol. 54, no.3, March 2007.

[13] A. Manoi, J.W. Pomeroy, N. Killat, M. Kuball, "Benchmarking of Thermal Boundary Resistance in AlGaIn/GaN HEMTs on SiC Substrates: Implications of the Nucleation Layer Microstructure", *IEEE electron device letters*, vol. 31, no.12, December 2010.